光学学报

混沌激光偏振度对同步质量影响的实验研究

申嘉皓[1]，狄呈震[1]，黄辉宇[1]，师天一[4]，王龙生[1,2*]，王安帮[1,3]，杨毅彪[1]，王云才[3]

[1]太原理工大学新型传感器与智能控制教育部/山西省重点实验室，山西 太原 030024；
[2]中国科学院长春光学精密机械与物理研究所应用光学国家重点实验室，吉林 长春 130033；
[3]广东工业大学广东省信息光子技术重点实验室，广东 广州 510006；
[4]大连理工大学光电工程与仪器学院，辽宁 大连 116024

摘要 对主从开环结构下，混沌激光偏振度对混沌同步质量的影响进行实验研究。在背靠背和 200 km 传输条件下，分析混沌激光偏振度以及同步质量的演变规律，发现随着距离和时间的增加，混沌激光偏振度逐渐减小，导致激光器的有效注入强度降低，进而削弱了注入锁定效应，恶化了主从混沌同步质量。增大注入强度可以提高同步质量对偏振度变化的容忍度，有助于实现稳定的长距离混沌激光同步。

关键词 激光器；光偏振度；混沌激光；混沌同步；混沌保密通信

中图分类号 TN248.4 **文献标志码** A **DOI**：10.3788/AOS230940

1 引 言

随着云计算、大数据、视频服务等新兴网络业务的发展，光纤通信流量呈现爆炸式增长，亟需发展高速光纤保密通信技术。基于混沌光同步的保密通信兼顾物理层安全、高速率、长距离、与光纤通信系统兼容等优点，被作为极具应用潜力的保密传输方式之一而受到广泛关注[1-3]。2005 年欧盟第五届科技框架计划 OCCULT 项目利用混沌半导体激光器在希腊雅典城域网中进行了距离为 120 km 的现场实验，实现了速率为 1 Gbit/s 的混沌保密传输[1]。2010 年 Larger 教授团队[4]利用混沌光电振荡器在法国贝桑松城 100 km 光纤链路中完成了 10 Gbit/s 混沌通信实验。

为了匹配现有城域网通信速率，国内外研究学者开展了混沌保密传输速率提升研究[5-14]，并取得了重要进展。义理林教授团队[15]利用光电振荡器作为混沌载波源并结合双二进制高阶调制实验实现了 100 km、30 Gbit/s 的混沌保密传输；随后，该团队在保证速率不变的前提下，结合相干检测将传输距离提升至 340 km[16]。江宁教授团队[17]将激光器混沌相位动态转换为强度动态以增加载波带宽，理论实现了 40 Gbit/s 的保密传输。闫连山教授团队[18]通过在混沌光电振荡器系统中引入神经网络，实验实现了 100 km、56 Gbit/s 的保密传输。本课题组通过增大激光器偏置电流提升混沌载波带宽，实验实现了 40 km、10 Gbit/s 的保密传输[19]；随后，提出基于光学 16QAM（正交幅度调制）与相干检测的混沌保密传输方案，模拟实现了 100 km、40 Gbit/s 的保密传输[20]。为了进一步提升保密传输速率，偏振复用是一种潜在方式。潘炜教授团队[21]通过选择 X 偏振光注入激光器，理论实现了偏振选择混沌同步。江宁教授团队、夏光琼教授团队[22-24]在理论上提出了基于垂直腔面发射激光器的混沌偏振复用保密传输方案。殷洪玺教授团队[25]利用传统光纤信道和激光混沌加密信道偏振复用，实验实现了 22.54 km、每通道传输速率为 1.25 Gbit/s 的信息传输。程孟凡教授团队[26]利用双偏振同向正交（IQ）调制器以及独立成分分析算法，实验实现了 100 km、60 Gbit/s 的混沌保密传输。闫连山教授团队[27]利用光电振荡器并结合偏振复用与盲解密算法，实验实现了 1040 km、112 Gbit/s 的混沌保密传输。

目前，长距离、高速的混沌偏振复用保密传输均是利用光电振荡器作为载波源，并结合后续算法解决偏振问题。相比之下，基于激光器的混沌偏振复用传输距离短、速率低，主要原因包括：1）现有偏振算法应用于激光混沌系统的可行性尚未被证明；2）混沌激光偏振度（DOP）限制同步质量，其影响规律尚不明晰。本文就混

收稿日期：2023-05-06；**修回日期**：2023-05-25；**录用日期**：2023-06-16；**网络首发日期**：2023-08-20

基金项目：国家自然科学基金（62035009，62105233）、山西省“1331 工程”重点创新团队、山西省重点研发计划国际合作项目（201903D421012）、中央引导地方科技发展基金（YDZJSX2021A009）、应用光学国家重点实验室开放基金（SKLAO2022001A09）、中物院创新发展基金（C-2023-CX20230030）

通信作者：*wanglongsheng@tyut.edu.cn

沌激光偏振度对同步质量的影响规律及优化方法进行了实验探索。结果表明，随着传输距离与时间的增加，混沌激光偏振度逐渐恶化，降低了激光器的有效注入强度与锁定效应[28]，导致同步质量下降，而通过增大注入强度可缓解偏振度恶化带来的同步质量下降问题。

2 实验装置

图 1 为单偏振态主从开环结构混沌同步的实验装置。首先，由主激光器镜面反馈产生的混沌激光通过掺铒光纤放大器进行功率放大后，经过偏振控制器和偏振分束器，以保证其线偏振态；然后，线偏振光通过 50∶50 耦合器被分为两束，一束作为主激光器混沌光探测端，另一束经过不同距离传输后，在接收端测量偏振分束器的输出端口功率，从而得到混沌激光偏振度的变化；最后，将混沌激光注入从激光器，实现单偏振态主从开环结构混沌同步。其中，经过长距离传输后，主从混沌同步类型为延时同步，延迟时间与传输距离成正比，例如：在经过 100 km 传输后，主从同步延时约为 500 μs；在经过 200 km 传输后，主从同步延时约为 1000 μs。实验中主激光器的阈值电流 I_{th} 为 9.7 mA，工作电流为 11.2 mA（$1.15I_{\mathrm{th}}$），工作温度为 23.7 ℃，其自由运行时的输出功率为 0.31 mW，主激光器通过镜面反馈产生混沌激光，反馈强度 K_{f} 为反馈光与激光器静态输出光的功率之比，为 5.2%。从激光器的阈值电流 I_{th} 为 10.2 mA，工作电流为 12.2 mA（$1.2I_{\mathrm{th}}$），工作温度为 28.8 ℃，自由运行时输出功率为 0.24 mW。需要指出的是：将工作电流设置在阈值电流附近，主要是为了获得小的弛豫振荡频率，主从激光器弛豫振荡频率分别为 2.8 GHz 和 2.7 GHz；实验中设置的温差较大，是为了获得合适的波长失谐，主从静态波长分别为 1547.298 nm 和 1547.226 nm，波长失谐为 −0.072 nm[29]。K_{j} 为由主激光器产生并注入从激光器的混沌激光和从激光器静态输出光的功率之比。背靠背（BTB）条件下实现主从 0.986 的同步性，此时 $K_{\mathrm{j}}=17.1\%$，200 km 传输后主从同步性为 0.962，此时 $K_{\mathrm{j}}=21.7\%$。

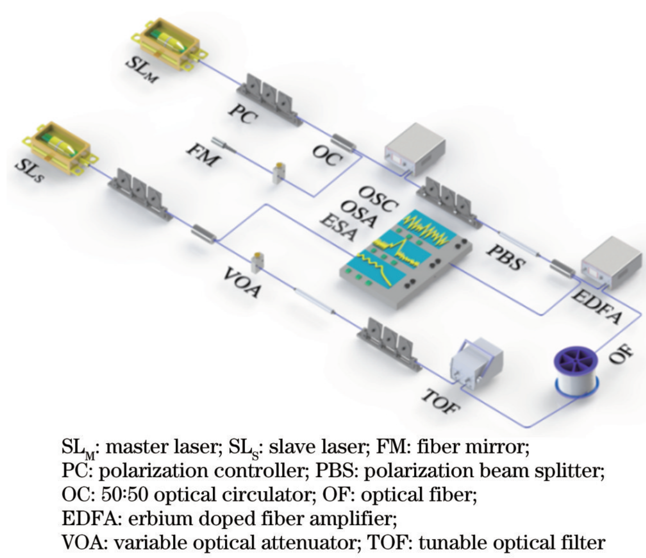

图 1 单偏振态主从开环结构混沌同步实验装置

Fig. 1 Experimental setup of chaos synchronization with single-polarization master-slave open-loop structure

主激光器和从激光器均为自研短腔分布式反馈（DFB）半导体激光器，掺铒光纤放大器（Amonics，AEDFA-PA-35-B-FA）的总增益超过 30 dB，最大噪声系数为 4.3 dB；可调谐光滤波器（EXFO，XTM-50）的滤波带宽为 6.25～625 GHz，滤波深度为 40 dB；光电探测器（Finisar，XPDV2120RA）的截止带宽为 50 GHz；光谱分析仪（YOKOGAWA，AQ6370D）的分辨率为 0.02 nm；频谱分析仪（Rohde and Schwarz，FSW-50）的带宽为 50 GHz；高速实时示波器（Lecroy，LABMASTER10ZI）的带宽为 36 GHz，采样率为 80 GSa/s。

3 实验结果

两个典型距离下单偏振态主从开环结构混沌同步结果如图 2 所示，其中图 2（a）、（b）所示为背靠背条件下主从混沌同步光谱和频谱，图 2（c）、（d）所示为传输 200 km 时主从混沌同步光谱和频谱。

主从混沌同步性采用互相关系数来定量表征，即

$$C_{\mathrm{C}}=\frac{\left\langle\left[P_{\mathrm{A}}(t-\tau_0)-\left\langle P_{\mathrm{A}}(t-\tau_0)\right\rangle\right]\left[P_{\mathrm{B}}(t)-\left\langle P_{\mathrm{B}}(t)\right\rangle\right]\right\rangle}{\sqrt{\left\langle\left[P_{\mathrm{A}}(t-\tau_0)-\left\langle P_{\mathrm{A}}(t-\tau_0)\right\rangle\right]^2\right\rangle\left\langle\left[P_{\mathrm{B}}(t)-\left\langle P_{\mathrm{B}}(t)\right\rangle\right]^2\right\rangle}},\tag{1}$$

式中：P_{A}、P_{B} 分别表示两束混沌激光的平均光功率；τ_0 表示两路混沌信号的相对时延；〈•〉表示取平均值。互相关系数的取值范围为 0～1，互相关系数越接近 1，说明主从混沌激光的同步性越高，而互相关系数越接近 0，则同步性越低。

图 3（a）、（b）所示为背靠背条件下的主从混沌同步时序和关联点图，图 3（c）、（d）所示为传输 200 km 条件下主从混沌同步时序、关联点图，选择以上两个典型距离作为特征距离进行分析对比。在背靠背条件下单偏振主从结构的混沌同步性为 0.986，经过 200 km 光纤传输后同步性为 0.962。

在这里，需要区分注入强度 K_{j} 和有效注入强度 $K_{\mathrm{j'}}$：注入强度 K_{j} 可通过光衰减器调节，而有效注入强度 $K_{\mathrm{j'}}$ 是指实际注入从激光器的光强，受混沌激光偏振

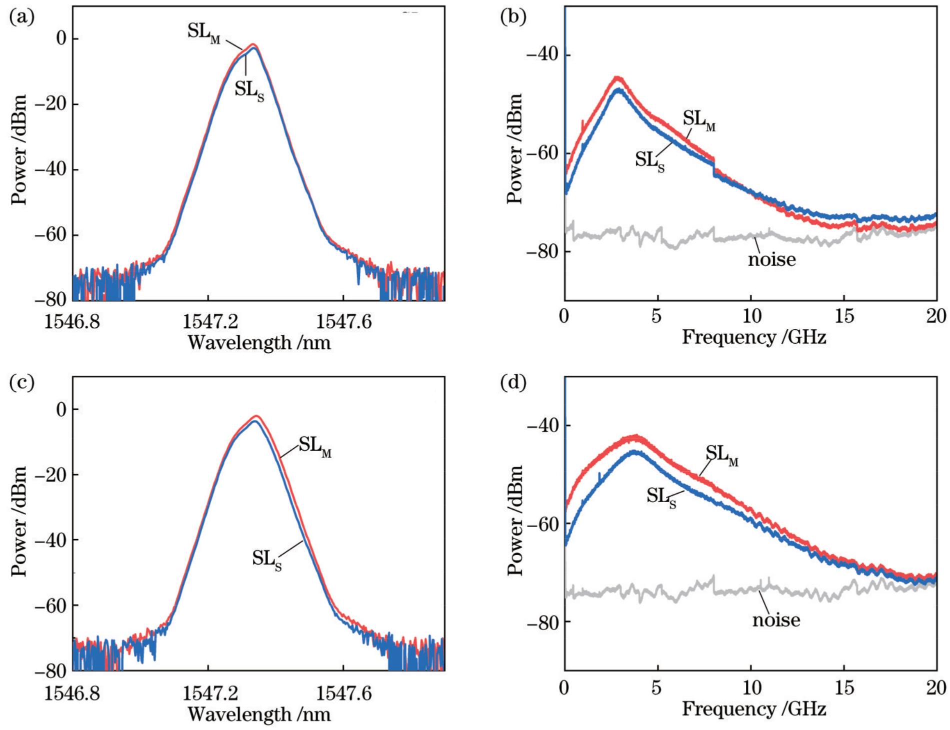

图 2　混沌同步光谱和频谱。(a)背靠背条件下的光谱；(b)背靠背条件下的频谱；(c)传输 200 km 时的光谱；(d)传输 200 km 时的频谱

Fig. 2　Optical and RF spectra of chaos synchronization. (a) Optical spectra at BTB; (b) RF spectra at BTB; (c) optical spectra at 200 km; (d) RF spectra at 200 km

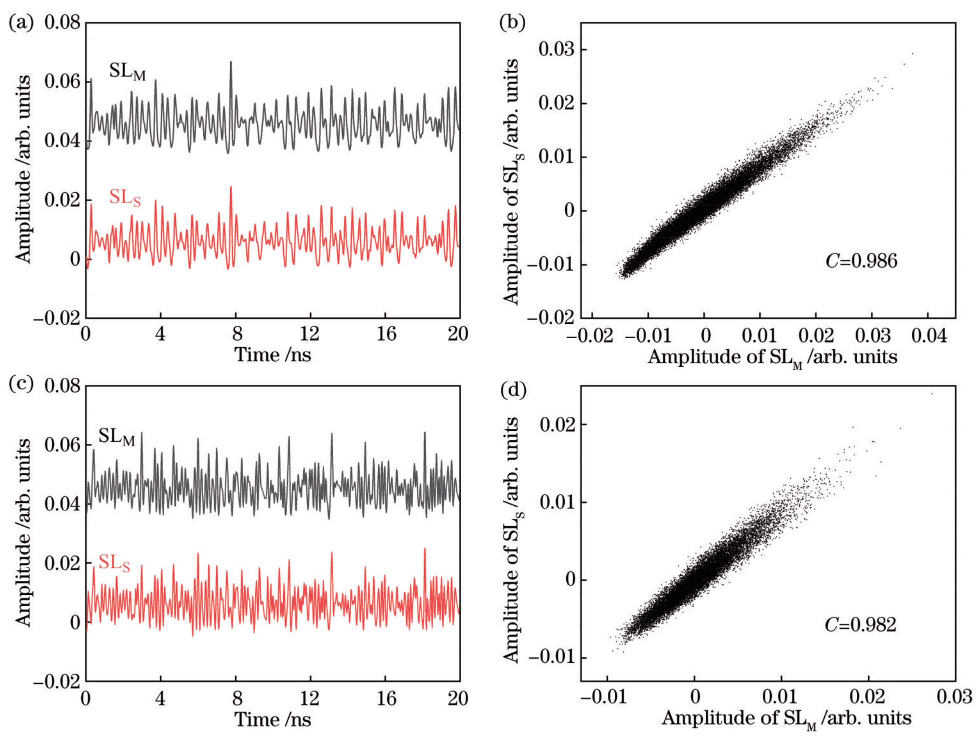

图 3　混沌同步时序图、关联点图。(a)背靠背条件下的时序图；(b)背靠背条件下的关联点图；(c)传输 200 km 的时序图；(d)传输 200 km 的关联点图

Fig. 3　Time series and correlation dot plots of chaos synchronization. (a) Time series at BTB; (b) correlation dot plot at BTB; (c) time series at 200 km; (d) correlation dot plot at 200 km

度的影响。

图 4 为背靠背和 200 km 情况下单偏振态主从开环结构混沌同步性随注入强度的变化曲线。可以看到：随着注入强度增大，主从激光器出现注入锁定，同

步性快速上升，当到达高质量同步性最低阈值0.90时同步性变化曲线的斜率下降，此时同步性上升速度减慢；在超过同步性临界饱和点（分别为0.980和0.960）后，主从同步性变化曲线趋于平稳。对比两条曲线发现，当主从激光器输出功率不变时，在相同注入强度下，传输距离长的主从同步性会变差，这是由色散以及其他非线性效应增强导致的，原因如下：随着传输距离增加，光纤色散会导致混沌波形展宽，同时入纤功率增加会导致非线性效应（自相位调制、交叉相位调制等）增强，造成信号失真，从而降低了混沌同步质量[30-31]。当主激光器混沌信号传输100 km时，前后同步性为0.984，主从同步性为0.973；当主激光器混沌信号传输200 km时，前后同步性为0.975，主从同步性为0.962。

在背靠背条件下选取初始同步性为0.90、0.980的2个特征同步性点，并在200 km条件下选取初始同步性为0.90、0.960的2个特征同步性点，其中同步性为0.90是高质量同步性的最低阈值，而同步性0.980、0.960是同步性的临界饱和点。

偏振度定量表征公式为

$$P=\frac{I_{\max}-I_{\min}}{I_{\max}+I_{\min}},\tag{2}$$

式中：$I_{\max}$表示混沌激光经过偏振分束器后初始功率大的一端的输出功率；$I_{\min}$表示经过偏振分束器后初始功率小的一端的输出功率。混沌激光的偏振度可以通过

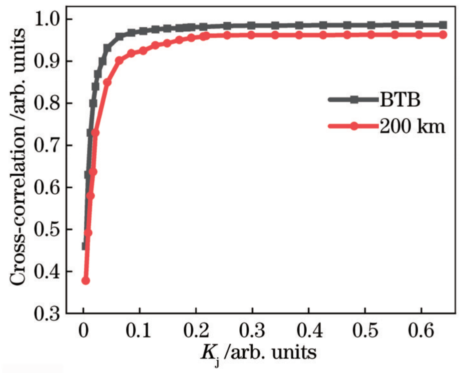

图4　背靠背和200 km时注入强度对同步性的影响

Fig. 4　Influence of injection strength on synchronization at BTB and 200 km

同时测量偏振分束器两个输出端口的功率结合式（2）计算得到，偏振度范围为−1～1。当偏振度趋于1时，只有注入从激光器的X偏振方向（与从激光器光场同向）的光功率不为0，垂直于Y偏振方向的光功率分量为0，此时即为最佳偏振度。

在背靠背和200 km条件下，选取初始同步性为0.90，通过调节偏振分束器前的偏振控制器改变主激光器混沌激光的偏振度，并研究其对于主从同步性的影响，结果如图5（a）、（c）所示。对比发现，随着距离增加，混沌同步性要想达到0.90，注入强度也要增大，这是因为经过长光纤传输后色散和非线性效应增强。在

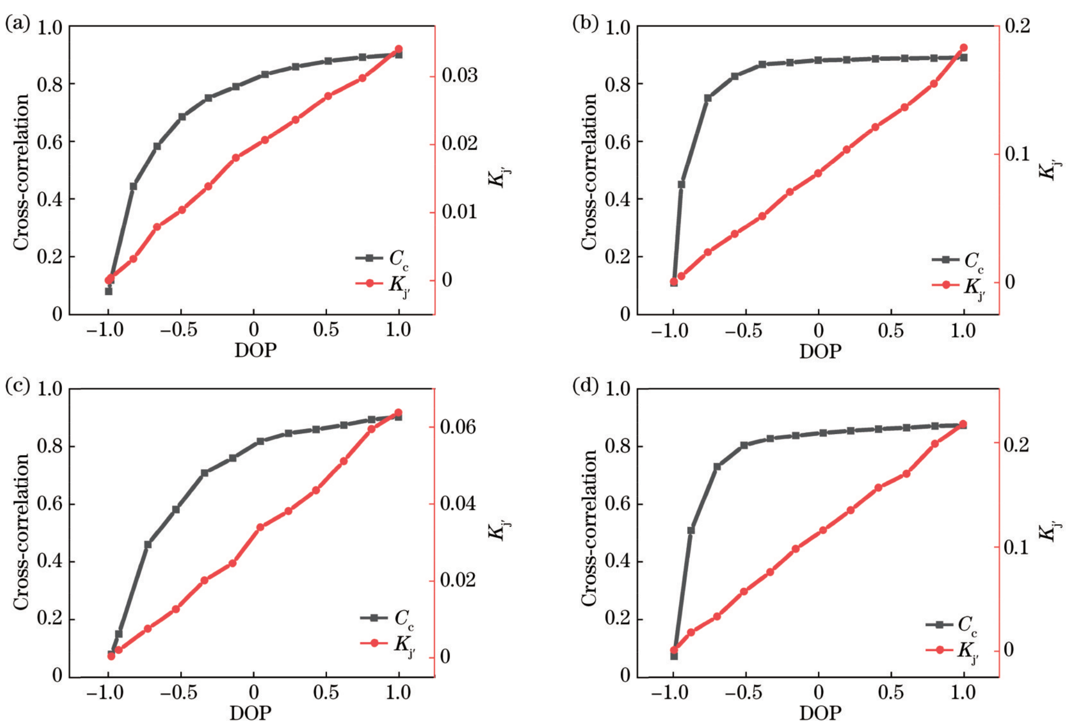

图5　偏振度对有效注入强度和同步性的影响。（a）背靠背条件下，C_{initial}=0.90；（b）背靠背条件下，C_{initial}=0.980；（c）200 km条件下，C_{initial}=0.90；（d）200 km条件下，C_{initial}=0.960

Fig. 5　Influence of DOP on effective injection strength and synchronization. (a) C_{initial}=0.90 at BTB; (b) C_{initial}=0.980 at BTB; (c) C_{initial}=0.90 at 200 km; (d) C_{initial}=0.960 at 200 km

偏振度从1恶化到−1的过程中，从激光器的注入效率首先受到影响，使得实际有效注入功率下降，注入锁定效应减弱，进而对主从同步质量产生影响。在背靠背和200 km条件下，选取初始同步性为0.980、0.960，通过调节偏振控制器改变偏振度，并研究其对于主从同步性的影响，结果如图5(b)、(d)所示。分别对比图5(a)、(b)和图5(c)、(d)可以发现：当初始同步性为0.90时，由于主从同步性随注入强度的变化曲线的斜率较大，因此主从同步性对有效注入功率变化的容忍度较低，偏振度从1恶化到−1的过程中同步性变化较快；当初始同步性为0.960、0.980时，同步性变化曲线趋于饱和，主从同步性对有效注入功率变化的容忍度变高，此时主从同步性先缓慢变化一段时间再快速降低。

在背靠背和200 km条件下，选取初始主从同步性为0.90，观察60 min内主激光器混沌激光偏振度的变化趋势和主从同步性的变化趋势，并间隔5 min记录一次，结果如图6(a)、(c)所示。可以看到：60 min内在背靠背条件下主激光器的单个偏振态的偏振度几乎没有变化，对实际有效注入强度的影响很小，所以主从同步性可保持在0.90；在200 km条件下，偏振度出现较大变化，此时从激光器的有效注入强度也出现明显变化，注入锁定效应被削弱，对应的主从同步性也相应下降。

在背靠背和200 km下，选取初始同步性为0.980、0.960，按上述步骤记录主激光器混沌激光的偏振度、有效注入强度和主从同步性的变化趋势，如图6(b)、(d)所示。在背靠背条件下，选取初始同步性为0.980，60 min内其偏振度、有效注入强度和主从同步性基本保持稳定；在200 km条件下，选取初始同步性为0.960，偏振度改变，并对有效注入强度产生较大影响，主从同步性也随之下降。另外，对比图6(c)、(d)可以发现，在200 km条件下当初始同步性为0.90时，60 min内同步性的下降趋势会比初始为0.960时更大些，这也是因为初始同步性为0.90时的同步性变化未趋于饱和，同步质量对偏振度和有效注入强度变化的容忍度较低，而初始同步性为0.960时的主从同步性随注入强度变化已经趋于饱和，同步质量的鲁棒性提高。

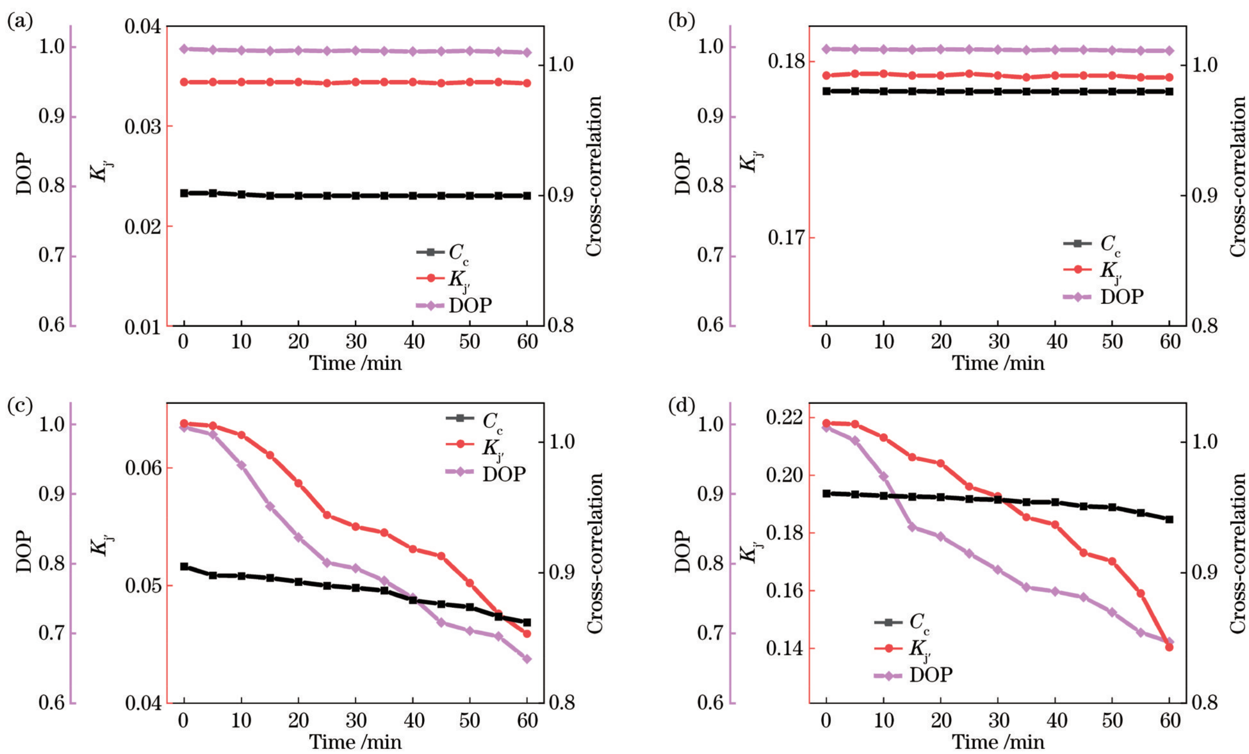

图6 60 min内偏振度、有效注入强度和同步性变化。(a) $C_{initial}$=0.90 at BTB；(b) $C_{initial}$=0.98 at BTB；(c) $C_{initial}$=0.90 at 200 km；(d) $C_{initial}$=0.96 at 200 km

Fig. 6 Trend of DOP, effective injection strength, and synchronization in 60 min. (a) $C_{initial}$=0.90 at BTB; (b) $C_{initial}$=0.980 at BTB; (c) $C_{initial}$=0.90 at 200 km; (d) $C_{initial}$=0.960 at 200 km

分别选取不同距离下同步性为0.90(高质量同步最低阈值)和同步性临界饱和点为初始状态，观测60 min内的混沌激光偏振度和同步性变化，如图7所示。同步性临界饱和点的选取如下：背靠背和50 km条件下初始同步性选取0.980，100 km条件下选取0.970，150 km和200 km条件下选取0.960，240 km和280 km分别选取0.950、0.940。

图7(a)、(c)所示分别为选取初始同步性0.90和同步性临界饱和点时，不同距离下最佳偏振度和60 min内偏振度变化后的状态。可以看到，同一距离

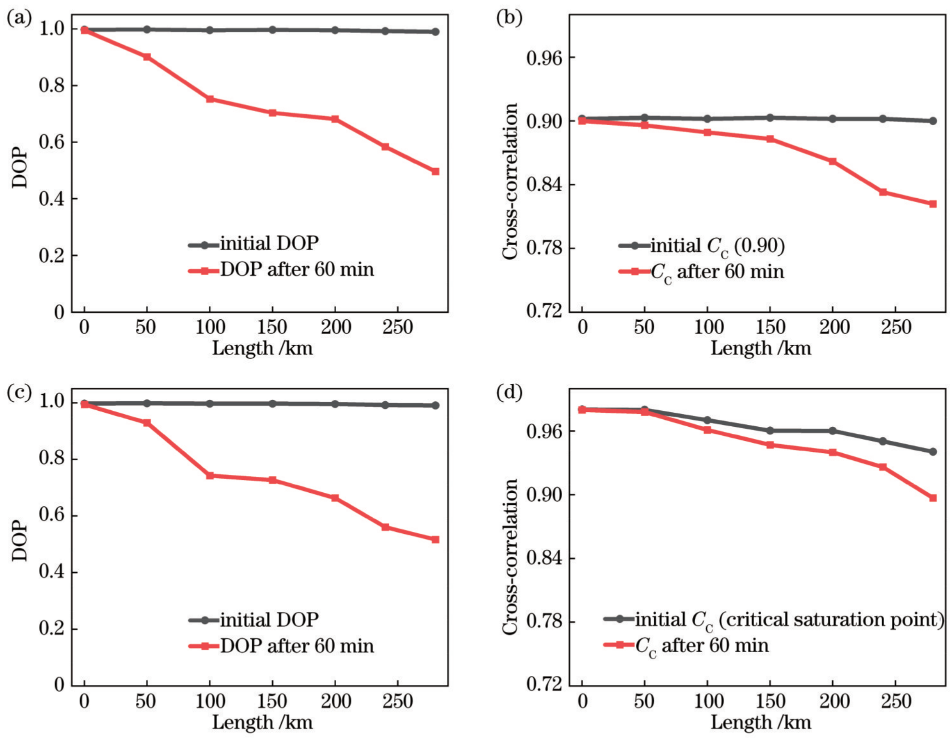

图 7 60 min 内距离变化对偏振度和同步性的影响。(a) C_{initial}=0.90 时偏振度变化趋势；(b) C_{initial}=0.90 时同步性的变化趋势；(c) C_{initial} 为同步性临界饱和点时偏振度的变化趋势；(d) C_{initial} 为同步性临界饱和点时同步性的变化趋势

Fig. 7 Influence of distance on DOP and synchronization in 60 min. (a) DOP trend at C_{initial}=0.90; (b) synchronization trend at C_{initial}=0.90; (c) DOP trend when C_{initial} is at critical saturation point; (d) synchronization trend when C_{initial} is at critical saturation point

下偏振度的变化程度接近，而不同距离的最佳偏振度范围为 0.99721～0.98961，60 min 内偏振度变化的范围为 0.99352～0.51661。图 7(b)展示了初始同步性为 0.90 时，不同距离下 60 min 内同步性的变化趋势，图 7(d)则展示了初始同步性为同步性临界饱和点时，不同距离下 60 min 内同步性的变化趋势。对比图 7(b)、(d)可知，在偏振度变化程度接近的情况下，当初始同步性为 0.90 时，同步质量对偏振度和有效注入强度变化的容忍度较低，其 60 min 内同步性下降趋势更明显。当传输距离为 280 km 时，初始同步性为临界饱和点 0.940，60 min 后同步性会下降至 0.897，减小了 4.57%；当初始同步性为 0.90 时，60 min 后同步性下降至 0.822，减小了 8.67%。由此可见，当初始同步性处于临界饱和点时，其长距离混沌激光同步更加稳定。

需要指出的是，混沌激光偏振度的恶化本质上来源于偏振态受到影响。影响偏振态的主要因素包括：1)光纤不均匀，存在形状缺陷；2)环境存在震动和温度变化等。针对光纤不均匀、存在形状缺陷的问题，需要优化光纤加工工艺；针对环境存在震动问题，可将实验系统放置于光学减震平台以降低震动的影响；针对温度变化的问题，可通过实验室中央空调来恒定温度。除此之外，实验中通常使用机械式偏振控制器调节偏振态，但随着传输距离和时间增加，其无法实时恢复偏振态，更有效的方式是利用偏振追踪器对偏振态进行实时自适应调节。

4 结　　论

对不同距离下混沌激光偏振度的变化及其对主从开环混沌同步质量的影响规律与优化方法进行探索。结果表明，随着距离增加，混沌激光偏振度恶化加剧：当经过 100 km、200 km 和 280 km 传输后，60 min 内的混沌激光偏振度分别下降了约 0.253、0.332 和 0.473。这将导致主激光器注入从激光器的有效光强度降低，进而恶化混沌同步质量。增大注入强度可以提高混沌同步对偏振度恶化的容忍度，改善同步鲁棒性。相关工作为实现基于偏振复用的高速、长距离混沌激光保密传输提供了参考。

参　考　文　献

[1] Argyris A, Syvridis D, Larger L, et al. Chaos-based communications at high bit rates using commercial fibre-optic links[J]. Nature, 2005, 438(7066): 343-346.

[2] Wang L S, Wang D M, Gao H, et al. Real-time 2.5-Gbit/s correlated random bit generation using synchronized chaos induced by a common laser with dispersive feedback[J]. IEEE Journal of Quantum Electronics, 2020, 56(1): 2000208.

[3] Gao H, Wang A B, Wang L S, et al. 0.75 Gbit/s high-speed classical key distribution with mode-shift keying chaos synchronization of Fabry-Perot lasers[J]. Light: Science & Applications, 2021, 10: 172.

[4] Lavrov R, Jacquot M, Larger L. Nonlocal nonlinear electro-optic phase dynamics demonstrating 10 Gb/s chaos communications[J]. IEEE Journal of Quantum Electronics, 2010, 46(10): 1430-1435.

[5] Xiang S Y, Pan W, Luo B, et al. Wideband unpredictability-enhanced chaotic semiconductor lasers with dual-chaotic optical injections[J]. IEEE Journal of Quantum Electronics, 2012, 48(8): 1069-1076.

[6] Wu J G, Wu Z M, Liu Y R, et al. Simulation of bidirectional long-distance chaos communication performance in a novel fiber-optic chaos synchronization system[J]. Journal of Lightwave Technology, 2013, 31(3): 461-467.

[7] Ai J Z, Wang L L, Wang J. Secure communications of CAP-4 and OOK signals over MMF based on electro-optic chaos[J]. Optics Letters, 2017, 42(18): 3662-3665.

[8] Li N Q, Susanto H, Cemlyn B, et al. Secure communication systems based on chaos in optically pumped spin-VCSELs[J]. Optics Letters, 2017, 42(17): 3494-3497.

[9] Fu Y D, Cheng M F, Jiang X X, et al. High-speed optical secure communication with an external noise source and an internal time-delayed feedback loop[J]. Photonics Research, 2019, 7(11): 1306-1313.

[10] Jiang N, Zhao A K, Xue C P, et al. Physical secure optical communication based on private chaotic spectral phase encryption/decryption[J]. Optics Letters, 2019, 44(7): 1536-1539.

[11] Yang Z, Yi L L, Ke J X, et al. Chaotic optical communication over 1000 km transmission by coherent detection[J]. Journal of Lightwave Technology, 2020, 38(17): 4648-4655.

[12] Fu Y D, Cheng M F, Shao W D, et al. Analog-digital hybrid chaos-based long-haul coherent optical secure communication[J]. Optics Letters, 2021, 46(7): 1506-1509.

[13] Gao Z S, Li Q H, Zhang L H, et al. 32 Gb/s physical-layer secure optical communication over 200 km based on temporal dispersion and self-feedback phase encryption[J]. Optics Letters, 2022, 47(4): 913-916.

[14] 李琼, 邓涛, 吴正茂, 等. 安全性增强的双向长距离混沌保密通信[J]. 中国激光, 2018, 45(1): 0106001.
Li Q, Deng T, Wu Z M, et al. Security-enhanced bidirectional long-distance chaos secure communication[J]. Chinese Journal of Lasers, 2018, 45(1): 0106001.

[15] Ke J X, Yi L L, Xia G Q, et al. Chaotic optical communications over 100-km fiber transmission at 30-Gb/s bit rate[J]. Optics Letters, 2018, 43(6): 1323-1326.

[16] Yang Z, Ke J X, Zhuge Q B, et al. Coherent chaotic optical communication of 30 Gb/s over 340-km fiber transmission via deep learning[J]. Optics Letters, 2022, 47(11): 2650-2653.

[17] Zhao A K, Jiang N, Liu S Q, et al. Generation of synchronized wideband complex signals and its application in secure optical communication[J]. Optics Express, 2020, 28(16): 23363-23373.

[18] Jiang L, Feng J C, Yan L S, et al. Chaotic optical communications at 56 Gbit/s over 100-km fiber transmission based on a chaos generation model driven by long short-term memory networks[J]. Optics Letters, 2022, 47(10): 2382-2385.

[19] Wang L S, Guo Y Y, Wang D M, et al. Experiment on 10-Gb/s message transmission using an all-optical chaotic secure communication system[J]. Optics Communications, 2019, 453: 124350.

[20] Wang L S, Mao X X, Wang A B, et al. Scheme of coherent optical chaos communication[J]. Optics Letters, 2020, 45(17): 4762-4765.

[21] 张伟利, 潘炜, 罗斌, 等. 偏振选择互注入半导体激光器的混沌同步[J]. 中国激光, 2007, 34(1): 55-60.
Zhang W L, Pan W, Luo B, et al. Chaos synchronization in polarization selective mutually coupled semiconductor lasers[J]. Chinese Journal of Lasers, 2007, 34(1): 55-60.

[22] Jiang N, Pan W, Luo B, et al. Bidirectional dual-channel communication based on polarization-division-multiplexed chaos synchronization in mutually coupled VCSELs[J]. IEEE Photonics Technology Letters, 2012, 24(13): 1094-1096.

[23] 邓伟, 夏光琼, 吴正茂. 基于双光反馈垂直腔面发射激光器的双信道混沌同步通信[J]. 物理学报, 2013, 62(16): 164209.
Deng W, Xia G Q, Wu Z M. Dual-channel chaos synchronization and communication based on a vertical-cavity surface emitting laser with double optical feedback[J]. Acta Physica Sinica, 2013, 62(16): 164209.

[24] 赵艳梅, 夏光琼, 吴加贵, 等. 基于1550 nm垂直腔面发射激光器的长距离双向双信道光纤混沌保密通信研究[J]. 物理学报, 2013, 62(21): 214206.
Zhao Y M, Xia G Q, Wu J G, et al. Investigation of bidirectional dual-channel long-distance chaos secure communication based on 1550 nm vertical-cavity surface-emitting lasers[J]. Acta Physica Sinica, 2013, 62(21): 214206.

[25] Dou X Y, Yin H X, Yue H H, et al. Experimental demonstration of polarization-division multiplexing of chaotic laser secure communications[J]. Applied Optics, 2015, 54(14): 4509-4513.

[26] Wu Y Q, Luo H W, Deng L, et al. 60 Gb/s coherent optical secure communication over 100 km with hybrid chaotic encryption using one dual-polarization IQ modulator[J]. Optics Letters, 2022, 47(20): 5285-5288.

[27] Jiang L, Pan Y, Yi A L, et al. Trading off security and practicability to explore high-speed and long-haul chaotic optical communication[J]. Optics Express, 2021, 29(8): 12750-12762.

[28] Murakami A, Shore K A. Chaos-pass filtering in injection-locked semiconductor lasers[J]. Physical Review A, 2005, 72(5): 053810.

[29] Someya H, Oowada I, Okumura H, et al. Synchronization of bandwidth-enhanced chaos in semiconductor lasers with optical feedback and injection[J]. Optics Express, 2009, 17(22): 19536-19543.

[30] Wang L S, Wang J L, Wu Y S, et al. Chaos synchronization of semiconductor lasers over 1040-km fiber relay transmission with hybrid amplification[J]. Photonics Research, 2023, 11(6): 953-960.

[31] 伍玉山, 王俊丽, 毛晓鑫, 等. 单跨光纤长距离混沌激光保真传输实验研究[J]. 中国激光, 2023, 50(5): 0506002.
Wu Y S, Wang J L, Mao X X, et al. Experiment on long-distance fidelity transmission of laser chaos over single-span optical fiber[J]. Chinese Journal of Lasers, 2023, 50(5): 0506002.

Experimental Research on Effect of Degree of Polarization of Chaotic Laser on Synchronization Quality

Shen Jiahao[1], Di Chengzhen[1], Huang Huiyu[1], Shi Tianyi[4], Wang Longsheng[1,2*], Wang Anbang[1,3], Yang Yibiao[1], Wang Yuncai[3]

[1]*Key Laboratory of Advanced Transducers and Intelligent Control System, Ministry of Education and Shanxi Province, College of Physics and Optoelectronics, Taiyuan University of Technology, Taiyuan* 030024, *Shanxi, China*;

[2]*State Key Laboratory of Applied Optics, Changchun Institute of Optics, Fine Mechanics and Physics, Chinese Academy of Sciences, Changchun* 130033, *Jilin, China*;

[3]*Guangdong Provincial Key Laboratory of Information Photonics Technology, College of Information Engineering, Guangdong University of Technology, Guangzhou* 510006, *Guangdong, China*;

[4]*College of Optoelectronic Engineering and Instrumentation Science, Dalian University of Technology, Dalian* 116024, *Liaoning, China*

Abstract

Objective Secure communication based on chaotic laser has received much attention in recent years because of its high speed, long distance, and compatibility with existing fiber-optic networks. Much effort has been devoted to improving the rate of chaotic secure communication by increasing chaos bandwidth or using higher-order modulation. Unfortunately, there still exists a rate gap between the chaotic secure communication and the current fiber-optic communication. Polarization division multiplexing of chaotic laser is a potential alternative to reduce the rate gap. The key to implementing the polarization division multiplexing-based chaotic secure communication is establishing high-quality chaos synchronization. However, the influences of polarization of chaotic laser, i. e. , the degree of polarization (DOP), on the chaos synchronization are not ascertained clearly. In this paper, the effects of DOP of chaotic laser on the synchronization quality are investigated experimentally, and the optimization methods and conditions are achieved for yielding high-quality and stable chaos synchronization. This work underlies the high-speed chaotic secure communication using polarization division multiplexing.

Methods Firstly, we generate a chaotic laser from the master laser subject to mirror optical feedback and use the polarization controller and polarization beam splitter to make the chaotic laser characterized with a single polarization. Then, we inject it unidirectionally into the slave laser over the fiber link to achieve the single-polarization master-slave open-loop chaos synchronization. The polarization controller can adjust the state of polarization of the chaotic laser, and the DOP can be analyzed quantitatively by detecting the power from the output ports of the polarization beam splitter. Based on this experimental system, we examine the evolution of DOP and analyze its effect on the synchronization quality over time for fiber links with different transmission distances, when the threshold point (0. 90) and the critical saturation point of high-quality synchronization are selected as the initial states. By changing the DOP of the chaotic laser in an experiment, we ascertain the effects of DOP on the effective injection strength and the quality of master-slave chaos synchronization firstly; then we analyze the evolution trend of DOP and its effect on the effective injection intensity and the quality of chaos synchronization within 60 minutes. Finally, the trend of DOP of the chaotic laser as a function of distance and time, as well as its effect on the quality of master-slave chaos synchronization are studied.

Results and Discussions We experimentally achieve master-slave chaos synchronization by injecting single-polarization chaotic laser from the master laser into the slave laser through a polarization beam splitter, and chaos synchronization with synchronization coefficients of 0. 986 and 0. 962 is achieved under back-to-back and 200 km scenarios, respectively (Figs. 2 and 3). By comparing the back-to-back and 200 km transmission scenarios, we find that the quality of master-slave synchronization degrades under 200 km transmission with the same injection strength (Fig. 4), which is due to the distortion of chaotic laser caused by chromatic dispersion and enhancement of nonlinear effects. It is also found that the DOP of chaotic laser changes with time after a long-distance transmission, which reduces the injection efficiency of the master laser to the slave laser (Figs. 5‒7). As a result, the effective injection strength is decreased, and the quality of master-slave chaos synchronization is degraded. In addition, we select the threshold point and the critical saturation point of high-quality synchronization as the initial states and observe the evolution of DOP and synchronization quality over time after transmission with different distances. It is found that under a similar variation of DOP and the same transmission distance, the chaos synchronization degrades less and is more stable for the initial state under the critical saturation point, compared with the initial state of the threshold point. It is noted that the deterioration of DOP originates mostly from the shape defect of fiber, as well as the vibration and temperature variation in the environment. Optimizing the fabrication technology of fiber, reducing vibration, and stabilizing temperature will all help to mitigate the deterioration of DOP. In addition, a polarization tracker can also be used to optimize the DOP in real time.

Conclusions In this paper, the evolution of DOP of chaotic laser and its effect on the chaos synchronization quality, as well as the corresponding optimization methods are explored experimentally in the master-slave open-loop configuration. Results show that the DOP of chaotic laser deteriorates gradually with the increase in transmission distance and time: the DOP is separately reduced by 0.253, 0.332, and 0.473 within 60 minutes when the chaotic laser is transmitted over 100 km, 200 km, and 280 km fiber links, respectively. The deterioration of DOP reduces the effective injection strength of the master laser to the slave laser and thus degrades the chaos synchronization quality. The enhancement of injection strength will increase the system tolerance to the variation of DOP and improve the robustness of chaos synchronization, affording a high-quality long-distance chaos synchronization. It is believed that this work paves the way for high-speed long-distance chaotic secure communication based on the polarization division multiplexing.

Key words lasers; degree of light polarization; chaotic laser; chaos synchronization; chaotic secure communication